

Naimark extension for the single-photon canonical phase measurement

Nicola Dalla Pozza

*Quantum Driving and Bio-complexity, Dipartimento di Fisica e Astronomia,
Università degli Studi di Firenze, I-50019 Sesto Fiorentino, Italy**

Matteo G. A. Paris

*Quantum Technology Lab, Dipartimento di Fisica 'Aldo Pontremoli',
Università degli Studi di Milano, I-20133 Milano, Italy†*

(Dated: August 5, 2019)

We address the implementation of the positive operator-valued measure (POVM) describing the optimal M -outcomes discrimination of the polarization state of a single photon. Initially, the POVM elements are extended to projective operators by Naimark theorem, then the resulting projective measure is implemented by a Knill-Laflamme-Milburn scheme involving an optical network and photon counters. We find the analytical expression of the Naimark extension and the detection scheme that realise it for an arbitrary number of outcomes $M = 2^N$.

I. INTRODUCTION

Quantum information processing with flying qubits, especially photons, has been extensively studied in the last decades, with applications in communication [1, 2], quantum key distribution (QKD) [3, 4], quantum networking [5–7] and universal quantum computing [8–10]. While remarkable results for communication and QKD have already been proved [11–14], there is great expectation for the medium-to-long-term realization of a quantum internet [15, 16], and possibly of a photonic quantum computer [17].

In all these scenarios, photons are used as qubit encoders and information carriers because of their ability to travel long distances with minimal decoherence. Information processing is performed at the encoding and decoding stage, and in intermediate stages as well (e.g. in repeaters [18, 19]) to implement quantum gates. Depending on the qubit encoding into the possible degrees of freedom, gates may have easy or more challenging implementations in terms of resources [20], with two-qubit gates being the hardest components to realize due to the small photon-photon coupling that can be obtained via matter-mediated processes [21].

Several theoretical and experimental proposals have been put forward [22–28], but the transition from theory to practice is not always straightforward. In this paper, we focus our attention on quantum measurements and consider a detection scheme which arises in optimal discrimination theory. The detection operators are described by an analytical expression, and we translate it into an optical scheme. We believe the steps undertaken in this paper are relevant in the framework of current technology and that they will prove useful for the implementation of other measurement schemes in linear optics quantum computing with discrete variables.

The most general description of a quantum measurement is provided by positive operator-valued measures (POVMs) acting on the Hilbert space of the systems under investigation. Mathematically speaking, a POVM is a resolution of identity made by sets of positive operators $\{\Pi_k\}$, $\sum_k \Pi_k = \mathbb{I}$. The cardinality of the POVM is not limited by the dimension of the Hilbert space and the operators $\{\Pi_k\}$ are not required to be projectors. POVMs have found useful applications in several fields of quantum information theory, e.g. in unambiguous quantum discrimination, where the optimal detection scheme may not correspond to a projective measurement.

Experimental realizations, however, always involve *observable* quantities, which strictly correspond to projective measures. Therefore, the challenge usually comes in finding an appropriate detection scheme to realize a given POVM. Fortunately, there is a canonical route to achieve this goal, which is provided by the Naimark theorem [29–33], ensuring that the POVM formulation may always be extended to a projective one, which may then be implemented experimentally. More explicitly, the Naimark theorem states that for any POVM $\{\Pi_k\}_{k \in \mathcal{K}}$ on the Hilbert space \mathcal{H}_S , generating a probability distribution $p(k) = \text{Tr}_S[\rho \Pi_k]$, $\forall \rho$, there exist a set of orthogonal projectors $\{P_k\}_{k \in \mathcal{K}}$ on the enlarged Hilbert space $\mathcal{H}_A \otimes \mathcal{H}_S$ and a pure state $|\omega\rangle \in \mathcal{H}_A$ such that

$$p(k) = \text{Tr}_S[\rho \Pi_k] = \text{Tr}_{AS}[\rho \otimes |\omega\rangle\langle\omega| P_k].$$

In this paper, we address the implementation of the POVM $\{\Pi_k\}$, $k = 0, 1, \dots, M - 1$ which acts on the Hilbert space of a two-level system, and describes the optimal M -outcomes discrimination of the polarization state of a single photon. The explicit expression is given by

$$\Pi_k = \frac{2}{M} |\psi_k\rangle\langle\psi_k| \quad (1)$$

$$|\psi_k\rangle = \frac{1}{\sqrt{2}} (e^{-i\frac{\pi}{M}k}|0\rangle + e^{i\frac{\pi}{M}k}|1\rangle). \quad (2)$$

Our strategy to solve the problem is the following: firstly, the POVM elements Π_k are extended to projective oper-

* nicola.dallapozza@unifi.it

† matteo.paris@fisica.unimi.it

ators upon exploiting the Naimark theorem; secondly the resulting projective measure is implemented by a Knill-Laflamme-Milburn scheme involving an optical network and photon counters. The key idea is to consider an interferometer with a single rail input mode to receive the input signal, and multiple output path modes, one for each outcome. Each of these output modes goes to photon counters, such that when we record a click we assign the corresponding outcome. In this way, we have found explicitly the Naimark extension and the detection scheme for an arbitrary number of outcomes $M = 2^N$, $N > 1$.

The paper is structured as follows. In Section II the Naimark theorem is introduced and the algorithm to evaluate the extension of the phase measurement is described. In Section III the application of the Naimark extension to the phase measurement of the polarization of a single photon is presented. In Section II A we give the corresponding expressions in the case of $M = 8$. The extension is factorized in a sequence of unitaries in Section III A, with Section III B considering the case of $M = 8$ in this instance. The implementation of the unitaries are provided in Section III C, and two different schemes for the phase measurement are designed in Sections III D and III E. Section IV closes the paper with some concluding remarks.

II. NAIMARK EXTENSION OF PHASE POVM

We are going to consider phase-measurements on a qubit. In particular, we consider measurements described by the POVM $\{\Pi_k\}$, where the k -th outcome, $k \in \{0, 1, \dots, M-1\}$, is associated with the phase value $\theta_k = k\frac{2\pi}{M}$. The number of outcomes M defines the resolution of the measurement scheme, and it may be arbitrarily high. The scheme we are going to discuss works for M being a power of 2, i.e. $M = 2^N$, $N \geq 1 \in \mathbb{N}$.

As a matter of fact, many different kind of phase measurements have been analysed and discussed, with the main goal of achieving optimal phase estimation. In this paper we study how to implement the phase measurement which is the solution of the following problem. Given the states

$$|\varphi_k\rangle = \frac{|0\rangle + e^{i\varphi_k}|1\rangle}{\sqrt{2}},$$

where $\varphi_k = \frac{2\pi}{M}k$, $k \in \{0, 1, \dots, M-1\}$, drawn with equal probability $\frac{1}{M}$, find the optimal POVM $\{\Pi_k\}$ that maximizes the probability of guessing correctly, i.e.

$$P_{\text{guessing}} = \sum_k P[\theta_k|\varphi_k] = \sum_k \langle \varphi_k | \Pi_k | \varphi_k \rangle. \quad (3)$$

The problem is well known because of the symmetry of the states, and the solution, which was found long ago [32], is the POVM in Eq. (1). This optimal POVM

may also be seen as an approximate *canonical phase-measurement*, that is, the measurement defined by the POVM $\{\Pi_\theta\}$, $\theta \in [0, 2\pi)$ defined in the standard basis as

$$\Pi_\theta = \frac{1}{2\pi} |\theta\rangle\langle\theta|, \quad |\theta\rangle = \sum_n e^{in\theta} |n\rangle. \quad (4)$$

When we restrict the Hilbert space to the subspace spanned by $|n\rangle = \{|0\rangle, |1\rangle\}$ and we discretize the outcome θ in the M values θ_k , we obtain the POVM $\{\Pi_k\}$ of Eq. (1). Note that each POVM element may be expressed in terms of the column vectors

$$|\psi_k\rangle = \frac{1}{\sqrt{2}} \begin{bmatrix} e^{-ik\frac{\pi}{M}} \\ e^{ik\frac{\pi}{M}} \end{bmatrix} \quad (5)$$

for $k = 0, 1, \dots, M-1$, and also as

$$\Pi_k = X_k X_k^\dagger, \quad X_k = \frac{1}{\sqrt{M}} \begin{bmatrix} e^{-ik\frac{\pi}{M}} \\ e^{ik\frac{\pi}{M}} \end{bmatrix}, \quad (6)$$

i.e., using the set of the *unnormalized* column vector X_k . Note also that the POVM elements are not orthogonal, except for $M = 2$, $\Pi_k \Pi_l \neq \Pi_k \delta_{k,l}$.

The POVM elements are operators on the original system Hilbert space \mathcal{H}_S and, according to the Naimark Theorem [29–33], may be implemented as a *projective measurement* in a larger Hilbert space \mathcal{H} , usually referred to as the *Naimark extension* of the POVM. Actually, the theorem ensures that a *canonical extension* exists amongst the infinite others, i.e., an implementation as an indirect measurement, where the system under investigation is coupled to an independently prepared probe system [34] and then only the probe is subject to a (projective) measurement [35–37], whose statistics mimic that of the POVM.

Here we look for a Naimark extension of the POVM $\{\Pi_k\}$ in Eq. (1) using a recursive algorithm designed in a previous paper [38]. The algorithm builds the projectors one by one, enlarging the size of the Hilbert space \mathcal{H} only when necessary. As we will see in a moment, the projectors have rank one and may be described in a matrix representation as $P_k = Z_k Z_k^\dagger$, with Z_k a column vector. Each projector must verify a set of orthogonality conditions, which translates to constraints on Z_k , i.e.

$$P_k P_l = 0, \quad k \neq l \quad \iff \quad Z_k^\dagger Z_l = 0, \quad (7)$$

as well as an idempotent condition,

$$(P_k)^2 = P_k \quad \iff \quad Z_k^\dagger Z_k = 1. \quad (8)$$

In addition, in order to be the extension of a POVM element, each projector P_k must satisfy

$$\Pi_k = \text{Tr}_A [P_k (\rho_A \otimes \mathbb{I}_S)], \quad (9)$$

which is the constraint required to evaluate the correct outcome probability in \mathcal{H}_S and in \mathcal{H} respectively, i.e.

$$\text{Tr}_S [\Pi_k \rho_S] = \text{Tr}_{AS} [P_k (\rho_A \otimes \rho_S)]. \quad (10)$$

In Eqs. (9) and in (10), we have introduced the enlarged Hilbert space \mathcal{H} given by the tensor product of an ancillary Hilbert space \mathcal{H}_A and the original Hilbert space \mathcal{H}_S , i.e. $\mathcal{H} = \mathcal{H}_A \otimes \mathcal{H}_S$. We have introduced also an auxiliary state ρ_A defined in \mathcal{H}_A , whose choice gives some degrees of freedom in building the extension. Following the suggestion of Helstrom [32], we use $\rho_A = |e_1^A\rangle\langle e_1^A|$, where $|e_1^A\rangle$ is the ancillary pure state whose column representation is the vector e_1 of the canonical basis with the appropriate size [39], i.e., with all the entries equal to zero except for the first one.

The recursive algorithm works by building the columns Z_k one at a time. In each column, the upper coefficients are set equal to X_k [40]. Then, the following coefficients are found by imposing the orthogonality condition (7) with the previously found Z_0, \dots, Z_{k-1} . Finally, the last coefficient is obtained by solving Eq. (8). All following coefficients are set to zero. If during the evaluation of a coefficient the provisional vector is already orthogonal to Z_l , $l < k$ or idempotent, it is not necessary to add another coefficient. This helps in reducing the growth in size of \mathcal{H} . The paper [38] actually finds a general expression for the coefficients to solve the orthogonal and idempotent constraints. The algorithm can be imple-

mented numerically to find the Naimark extension of the POVM $\{\Pi_k\}$. However, an analytical expression for the projectors for arbitrarily high M can be found when employing the order $Z_0, Z_{M/2}, Z_1, Z_{M/2+1}, \dots, Z_{M-1}$ for their evaluation. The projectors are hence extended in pairs evaluating Z_k and $Z_{k+M/2}$ for $k = 0, \dots, M/2 - 1$, resulting in the overall expressions of Eq. (12). To better illustrate how the recursive algorithm works, we show the case for $M = 8$ in the Section II A.

As expected, the first two coefficients are X_k . Then, $2(k+1)$ coefficients are defined, followed by zero entries that pad the vector up to the size of M . For $k = M/2 - 1$ and $k = M - 1$ the last coefficients (which would overflow the length of M) are zeros, so that $Z_{M/2-1}$ and Z_{M-1} can be truncated to the correct length. The columns Z_k can be packed in the $M \times M$ matrix Z ,

$$Z = [Z_0 \ Z_{M/2} \ Z_1 \ Z_{M/2+1} \ \dots \ Z_{M/2-1} \ Z_{M-1}] \quad (11)$$

and Eqs. (7), (8) can be checked analytically or numerically to verify $Z^\dagger \cdot Z = Z \cdot Z^\dagger = I$. As an example, we evaluate Z for $M = 8$ in Section II A and report it in Eq. (13). Expression (12) may be proved by induction.

$$Z_k = \begin{bmatrix} \frac{e^{-i\frac{k}{M}\pi}}{\sqrt{M}} \\ \frac{e^{i\frac{k}{M}\pi}}{\sqrt{M}} \\ -\frac{2}{\sqrt{M(M-2)}} \cos\left(\frac{k}{M}\pi\right) \\ -\frac{2}{\sqrt{M(M-2)}} \sin\left(\frac{k}{M}\pi\right) \\ -\frac{2}{\sqrt{(M-2)(M-4)}} \cos\left(\frac{k-1}{M}\pi\right) \\ -\frac{2}{\sqrt{(M-2)(M-4)}} \sin\left(\frac{k-1}{M}\pi\right) \\ \vdots \\ -\frac{2}{\sqrt{(M-2k+2)(M-2k)}} \cos\left(\frac{1}{M}\pi\right) \\ -\frac{2}{\sqrt{(M-2k+2)(M-2k)}} \sin\left(\frac{1}{M}\pi\right) \\ \sqrt{\frac{M-2k-2}{M-2k}} \\ 0 \\ 0 \\ \vdots \\ 0 \end{bmatrix}, \quad Z_{k+M/2} = \begin{bmatrix} \frac{e^{-i\frac{k+M/2}{M}\pi}}{\sqrt{M}} \\ \frac{e^{i\frac{k+M/2}{M}\pi}}{\sqrt{M}} \\ \frac{2}{\sqrt{M(M-2)}} \sin\left(\frac{k}{M}\pi\right) \\ -\frac{2}{\sqrt{M(M-2)}} \cos\left(\frac{k}{M}\pi\right) \\ \frac{2}{\sqrt{(M-2)(M-4)}} \sin\left(\frac{k-1}{M}\pi\right) \\ -\frac{2}{\sqrt{(M-2)(M-4)}} \cos\left(\frac{k-1}{M}\pi\right) \\ \vdots \\ \frac{2}{\sqrt{(M-2k+2)(M-2k)}} \sin\left(\frac{1}{M}\pi\right) \\ -\frac{2}{\sqrt{(M-2k+2)(M-2k)}} \cos\left(\frac{1}{M}\pi\right) \\ 0 \\ \sqrt{\frac{M-2k-2}{M-2k}} \\ 0 \\ \vdots \\ 0 \end{bmatrix} \quad (12)$$

A. Recursive evaluation of Z_k for $M = 8$

In this section we illustrate how the recursive algorithm presented in [38] builds the columns of Z for $M = 8$. The procedure can be followed by looking at the columns of Eq. (13), which represent the resulting matrix.

As anticipated in Section II, the columns are evaluated one at a time starting from Z_0 and following the

order of Eq. (11). In Z_0 , the first two coefficients are $X_0 = [1/\sqrt{M}, 1/\sqrt{M}]^T$. Then, the next coefficient is obtained by imposing the condition that the overall Z_0 has unitary norm, as in Eq. (8). These three coefficients will be extended and padded with zeros once the final length is known.

For the second column, which corresponds to Z_4 , the first two coefficients are $X_4 = [-i/\sqrt{M}, i/\sqrt{M}]^T$. The

following one is obtained by imposing the orthogonality constraint (7) with Z_0 , which gives a zero coefficient in the third item. The next coefficient is obtained from (8) imposing the unit norm.

The third column, which correspond to Z_1 , is evaluated with the same procedure. The first two coefficients are $X_1 = [e^{-i\pi/8}/\sqrt{M}, e^{i\pi/8}/\sqrt{M}]^T$. The following coefficients are obtained from the orthogonality constraint with Z_0 and Z_4 , obtaining $-2\cos(\pi/8)/\sqrt{(M-2)M}$ and $-2\sin(\pi/8)/\sqrt{(M-2)M}$, respectively. The following coefficient is obtained again from the idempotent con-

straint (8).

The recursive procedure continues in the same way for the remaining columns, first by copying the coefficients of X_k , then by imposing the orthogonality constraint (7) with all the previous columns, and finally evaluating the last coefficient by the idempotent constraint (8).

Note that while with this procedure up to $M+2$ coefficients may be evaluated for each column, the last coefficients of the last two columns are zeros since $M=8$, and the columns can be truncated to the correct length of $M=8$.

$$Z = \begin{bmatrix} \frac{1}{\sqrt{M}} & -\frac{i}{\sqrt{M}} & \frac{e^{-i\pi/8}}{\sqrt{M}} & \frac{e^{-i5\pi/8}}{\sqrt{M}} & \frac{e^{-i2\pi/8}}{\sqrt{M}} & \frac{e^{-i6\pi/8}}{\sqrt{M}} & \frac{e^{-i3\pi/8}}{\sqrt{M}} & \frac{e^{-i7\pi/8}}{\sqrt{M}} \\ \frac{1}{\sqrt{M}} & \frac{i}{\sqrt{M}} & \frac{e^{i\pi/8}}{\sqrt{M}} & \frac{e^{i5\pi/8}}{\sqrt{M}} & \frac{e^{i2\pi/8}}{\sqrt{M}} & \frac{e^{i6\pi/8}}{\sqrt{M}} & \frac{e^{i3\pi/8}}{\sqrt{M}} & \frac{e^{i7\pi/8}}{\sqrt{M}} \\ \sqrt{\frac{M-2}{M}} & 0 & -\frac{2\cos(\pi/8)}{\sqrt{(M-2)M}} & \frac{2\sin(\pi/8)}{\sqrt{(M-2)M}} & -\frac{2\cos(2\pi/8)}{\sqrt{M(M-2)}} & \frac{2\sin(2\pi/8)}{\sqrt{M(M-2)}} & -\frac{2\cos(3\pi/8)}{\sqrt{M(M-2)}} & \frac{2\sin(3\pi/8)}{\sqrt{M(M-2)}} \\ 0 & \sqrt{\frac{M-2}{M}} & -\frac{2\sin(\pi/8)}{\sqrt{(M-2)M}} & -\frac{2\cos(\pi/8)}{\sqrt{(M-2)M}} & -\frac{2\sin(2\pi/8)}{\sqrt{M(M-2)}} & -\frac{2\cos(2\pi/8)}{\sqrt{M(M-2)}} & -\frac{2\sin(3\pi/8)}{\sqrt{M(M-2)}} & -\frac{2\cos(3\pi/8)}{\sqrt{M(M-2)}} \\ 0 & 0 & \sqrt{\frac{M-4}{M-2}} & 0 & -\frac{2\cos(\pi/8)}{\sqrt{(M-2)(M-4)}} & \frac{2\sin(\pi/8)}{\sqrt{(M-2)(M-4)}} & -\frac{2\cos(2\pi/8)}{\sqrt{(M-2)(M-4)}} & \frac{2\sin(2\pi/8)}{\sqrt{(M-2)(M-4)}} \\ 0 & 0 & 0 & \sqrt{\frac{M-4}{M-2}} & -\frac{2\sin(\pi/8)}{\sqrt{(M-2)(M-4)}} & -\frac{2\cos(\pi/8)}{\sqrt{(M-2)(M-4)}} & -\frac{2\sin(2\pi/8)}{\sqrt{(M-2)(M-4)}} & -\frac{2\cos(2\pi/8)}{\sqrt{(M-2)(M-4)}} \\ 0 & 0 & 0 & 0 & \sqrt{\frac{M-6}{M-4}} & 0 & -\frac{2\cos(\pi/8)}{\sqrt{(M-4)(M-6)}} & \frac{2\sin(\pi/8)}{\sqrt{(M-4)(M-6)}} \\ 0 & 0 & 0 & 0 & 0 & \sqrt{\frac{M-6}{M-4}} & -\frac{2\sin(\pi/8)}{\sqrt{(M-4)(M-6)}} & -\frac{2\cos(\pi/8)}{\sqrt{(M-4)(M-6)}} \\ 0 & 0 & 0 & 0 & 0 & 0 & \sqrt{\frac{M-8}{M-6}} & 0 \\ 0 & 0 & 0 & 0 & 0 & 0 & 0 & \sqrt{\frac{M-8}{M-6}} \end{bmatrix} \quad (13)$$

III. PHASE-MEASUREMENT ON A SINGLE PHOTON

Let us denote by ρ_S the state of the qubit, defined on a two-level system representing the *single rail polarization encoding*, that is, identifying the logical system-basis $\{|0\rangle_L, |1\rangle_L\}$ with the polarization modes $|0\rangle_L = |H\rangle = a_H^{\dagger(m)}|0\rangle$, $|1\rangle_L = |V\rangle = a_V^{\dagger(m)}|0\rangle$. Operators $a_H^{\dagger(m)}$, $a_V^{\dagger(m)}$ are the creation operators of the polarization modes on the m -th path and $|0\rangle$ is the vacuum state. In this case the optical state is defined on a *single* path, as opposed to the *dual rail* encoding which employs the m -th and n -th spatial modes to define the logical basis $|0\rangle_L = |10\rangle_{mn} = a^{\dagger(m)}|00\rangle_{mn}$ and $|1\rangle_L = |01\rangle_{mn} = a^{\dagger(n)}|00\rangle_{mn}$.

Note that even though our system qubit is defined with the single rail polarization encoding, in the following we will also employ the dual rail encoding when speaking about the implementation scheme of the phase measurement. In that framework, we will denote the mode number in the superscript, while making the polarization explicit in the subscript.

Let us start by summarising the key idea behind our detection scheme. We implement the Naimark extension of the POVM by an optical network that receives the

quantum state ρ_S to be measured as input, and (probabilistically) outputs a single photon towards an array of photon counters. Each detector is associated with an outcome, corresponding to a click in a specific detector. In the ideal case of no losses in the network, and no detector noise, every time we send ρ_S into the optical network we always get one and only one click. In this respect, our scheme resembles the KLM scheme for measurements [8] since the measurement device is implemented with a unitary rotation followed by a set of projectors. In our case the overall projectors P_k to be applied on $\rho_A \otimes \rho_S$ can be obtained as $P_k = Z|e_k^{\mathcal{H}}\rangle\langle e_k^{\mathcal{H}}|Z^\dagger$, where $|e_k^{\mathcal{H}}\rangle$ is the state defined in \mathcal{H} with column representation of the k -th element of the canonical basis. Since

$$\text{Tr}[P_k \rho_A \otimes \rho_S] = \text{Tr}[(Z^\dagger \rho_A \otimes \rho_S Z) |e_k^{\mathcal{H}}\rangle\langle e_k^{\mathcal{H}}|], \quad (14)$$

the unitary rotation is defined by Z^\dagger and implemented with the optical network, while the projector $|e_k^{\mathcal{H}}\rangle\langle e_k^{\mathcal{H}}|$ is implemented with a photon counter on the k -th output mode.

A. Decomposition of the unitary Z^\dagger

The unitary Z^\dagger can be decomposed as a product of simpler unitary rotations [41] usually referred to as *Givens Rotations* (GR), i.e., a rotation in the plane spanned by two coordinates axes, often employed to zero out a particular entry in a vector. Section III C describes how to implement each GR, so that the overall sequence realizes the interferometer associated with Z^\dagger . GR have a matrix representation that looks like the identity matrix, with the exception of the coefficients on two rows and two columns, which define the mixing between the two.

We define such an $M \times M$ matrix as

$$W(u, v, \omega) = \begin{pmatrix} 1 & 0 & u & v & 0 \\ 0 & \ddots & 0 & 0 & 0 \\ 0 & 0 & \cos(\omega) & \sin(\omega) & 0 \\ 0 & 0 & -\sin(\omega) & \cos(\omega) & 0 \\ 0 & 0 & 0 & 0 & 1 \end{pmatrix} \begin{matrix} u \\ v \end{matrix} \quad (15)$$

with u, v the indices of the rows and columns being mixed, and ω a parameter defining the mixing. We define

also the matrix $S(u, \phi)$

$$S(u, \phi) = \begin{pmatrix} & & & u & \\ 1 & 0 & 0 & 0 & 0 \\ 0 & \ddots & & \vdots & \\ 0 & & 1 & 0 & 0 \\ 0 & \dots & 0 & e^{-i\phi} & 0 \\ 0 & 0 & 0 & 0 & 1 \end{pmatrix} \begin{matrix} u \end{matrix}, \quad (16)$$

which corresponds to a phase shift on the u -th vector of the basis.

In decomposing Z^\dagger we take advantage of its structure, which is almost lower-triangular due to the zero padding of Z_k to reach the length of M coefficients (see for instance the structure of Z in Eq. (13) in the example in Section II A). For further details on the decomposition of Z^\dagger are reported in Section III B.

A pattern in the sequence of unitaries W and S emerges, suggesting an analytical expression for the decomposition for any M (see for instance Eq. (17)). In fact, with the exception of $S(2, \pi/2)$ and $W(1, 2, \pi/4)$, the GR can be grouped in triplets of unitaries where the u, v indices act on the same group, e.g. $\{5, 7, 6, 8\}$, $\{3, 4, 5, 6\}$ or $\{1, 2, 3, 4\}$. The parameter ω also shows a pattern in its value, i.e. it has the same value in the first two GR of the triplet and it has the same value in the third GR amongst different triplets. These patterns have a direct effect on the physical realization of Z^\dagger decomposition (see Section III C).

$$\begin{aligned} Z^\dagger = & W\left(7, 8, \pi + \frac{\pi}{M}\right) \cdot W\left(6, 8, \arctan \sqrt{\frac{M-6}{2}}\right) \cdot W\left(5, 7, \arctan \sqrt{\frac{M-6}{2}}\right) \\ & \cdot W\left(5, 6, \pi + \frac{\pi}{M}\right) \cdot W\left(4, 6, \arctan \sqrt{\frac{M-4}{2}}\right) \cdot W\left(3, 5, \arctan \sqrt{\frac{M-4}{2}}\right) \\ & \cdot W\left(3, 4, \pi + \frac{\pi}{M}\right) \cdot W\left(2, 4, \arctan \sqrt{\frac{M-2}{2}}\right) \cdot W\left(1, 3, \arctan \sqrt{\frac{M-2}{2}}\right) \\ & \cdot S\left(2, \frac{\pi}{2}\right) \cdot W\left(1, 2, \frac{\pi}{4}\right) \end{aligned} \quad (17)$$

Expression (17) can be easily checked by multiplying it by Z and obtaining the identity matrix.

B. Decomposition of Z for $M = 8$

In this section we describe more in detail how the decomposition of Z^\dagger can be obtained. We will consider the case of $M = 8$, which is reported in Eq. (17).

We start from the corresponding matrix Z , whose expression is reported in Eq. (13). This matrix is unitary, and therefore can be decomposed as a sequence of GR

[41]. To find this decomposition, a handy procedure is to left-multiply Z by W, S until we obtain the identity matrix. In short, we should multiply Z by GR that nullify the off-diagonal entries. The sequence of W, S then corresponds to the decomposition we are looking for.

To simplify the procedure, we first multiply Z by $W_0 = W(1, 2, \pi/4)$ and $S_0 = S(2, \pi/2)$ to convert the complex entries in the first two rows of Z into their corresponding

real and imaginary parts. The matrix becomes

$$S_0 \cdot W_0 \cdot Z = \begin{bmatrix} \frac{\sqrt{2}}{\sqrt{M}} & 0 & \frac{\sqrt{2} \cos(\pi/M)}{\sqrt{M}} & \dots \\ 0 & \frac{\sqrt{2}}{\sqrt{M}} & \frac{\sqrt{2} \sin(\pi/M)}{\sqrt{M}} & \\ \sqrt{\frac{M-2}{M}} & 0 & -\frac{2 \cos(\pi/M)}{\sqrt{(M-2)M}} & \\ 0 & \sqrt{\frac{M-2}{M}} & -\frac{2 \sin(\pi/M)}{\sqrt{(M-2)M}} & \\ 0 & 0 & \sqrt{\frac{M-4}{M-2}} & \\ \vdots & & & \ddots \end{bmatrix}. \quad (18)$$

We can then focus on nulling the entry below the diagonal. We need a GR for each of the entries in the first and second columns, $W_1 = W(1, 3, \omega_{13})$ and $W_2 = W(2, 4, \omega_{24})$ respectively, with $\omega_{13} = \omega_{24} = \arctan(\sqrt{(M-2)/2})$. We then obtain

$$W_2 \cdot W_1 \cdot S_0 \cdot W_0 \cdot Z = \begin{bmatrix} 1 & 0 & 0 & 0 & \dots \\ 0 & 1 & 0 & 0 & \\ 0 & 0 & \frac{\sqrt{2} \cos(\frac{\pi}{M})}{\sqrt{M-2}} & -\frac{\sqrt{2} \sin(\frac{\pi}{M})}{\sqrt{M-2}} & \\ 0 & 0 & \frac{\sqrt{2} \sin(\frac{\pi}{M})}{\sqrt{M-2}} & \frac{\sqrt{2} \cos(\frac{\pi}{M})}{\sqrt{M-2}} & \\ 0 & 0 & \sqrt{\frac{M-4}{M-2}} & 0 & \\ 0 & 0 & 0 & \sqrt{\frac{M-4}{M-2}} & \\ \vdots & & & & \ddots \end{bmatrix}. \quad (19)$$

Note that at this point all the off-diagonal entries in the first and second rows, as well as those in the first and second columns are zero.

If we then multiply the matrix by $W_3 = W(3, 4, \pi + \pi/M)$ to nullify the first off-diagonal entry in the fourth row, we obtain a matrix that resembles (18) except for $M-2$ in place of M , i.e.

$$W_3 \cdot W_2 \cdot W_1 \cdot S_0 \cdot W_0 \cdot Z = \begin{bmatrix} 1 & 0 & 0 & 0 & \dots \\ 0 & 1 & 0 & 0 & \\ 0 & 0 & \frac{\sqrt{2}}{\sqrt{M-2}} & 0 & \\ 0 & 0 & 0 & \frac{\sqrt{2}}{\sqrt{M-2}} & \\ 0 & 0 & \sqrt{\frac{M-4}{M-2}} & 0 & \\ 0 & 0 & 0 & \sqrt{\frac{M-4}{M-2}} & \\ \vdots & & & & \ddots \end{bmatrix}. \quad (20)$$

The multiplication by $W_3 \cdot W_2 \cdot W_1$ has effectively nullified the left off-diagonal entries in the second and third rows of $S_0 \cdot W_0 \cdot Z$. From here on, we can find triplets of GR $\{W_6, W_5, W_4\}$ that acts like $\{W_3, W_2, W_1\}$ to nullify the left off-diagonal entries in rows 5, 6. This procedure can be repeated for the remaining rows and gives the pattern of GR triplets in the decomposition (17).

Once we obtain the final identity matrix, the product of the GR employed $W_9 \cdot W_8 \dots W_3 \cdot W_2 \cdot W_1 \cdot S_0 \cdot W_0$ is a decomposition of Z^\dagger . The decomposition works for arbitrarily high values of M since the matrix Z has the same structure.

C. Physical realization of Givens Rotations

Without loss of generality, we can consider the measurement of $\rho_S = |\varphi^S\rangle\langle\varphi^S|$, with $|\varphi^S\rangle$ being a single-photon state,

$$|\varphi^S\rangle = \frac{|0\rangle_L + e^{i\varphi}|1\rangle_L}{\sqrt{2}} = \frac{a_H^\dagger(1) + e^{i\varphi}a_V^\dagger(1)}{\sqrt{2}}|0\rangle, \quad (21)$$

and $\varphi \in [0, 2\pi)$ an unknown phase to be estimated. Again, $a_H^\dagger(1)$ and $a_V^\dagger(1)$ are the creator operators for the first path mode, for the horizontal and vertical mode respectively. In the case of a mixed state, the result of the phase measurement follows by linearity from the measurement of the eigenvectors of ρ_S .

To define the vector representation of the state in the enlarged Hilbert space \mathcal{H} , we collect the coefficients of the creation operators $a_H^\dagger(m)$, $a_V^\dagger(m)$ and stack them in order in a column. For instance, the input quantum state (21) is represented as

$$|\varphi^{AS}\rangle = |e_1^A\rangle \otimes |\varphi^S\rangle \rightarrow \begin{bmatrix} 1 \\ \frac{\sqrt{2}}{2} \\ \frac{e^{i\varphi}}{\sqrt{2}} \\ 0 \\ \vdots \\ 0 \end{bmatrix} \quad (22)$$

because the coefficients of $a_H^\dagger(1)$, $a_V^\dagger(1)$ are placed in the first two items in the column representation, while the zeros are the coefficients of $a_H^\dagger(m)$, $a_V^\dagger(m)$, $m > 1$.

This representation is useful because in the Hilbert space spanned by the polarizations of a single photon on multiple modes, the mixing of n optical modes is represented by a $n \times n$ unitary matrix [42]. As a consequence, the states that define the canonical basis in this representation and in the unitary Z^\dagger are single-photon states of some polarization and path modes. The auxiliary state $|e_1^A\rangle$ is just the tensor product of many vacuum states corresponding to multiple modes.

In this Hilbert space the converse also holds, i.e., any unitary transformation can be achieved with a set of passive devices such as beam splitters, polarizing beam splitters, waveplates and mirrors [43]. We will leverage this result to provide a possible realization for the unitaries $S(u, \phi)$ and $W(u, v, \omega)$.

The unitary $S(u, \phi)$ can be realized with a waveplate of the appropriate thickness where the fast axis is aligned with the horizontal mode and the slow axis with the vertical mode. In this way, the vertical mode gains a phase shift equal to $-\phi$ with respect to the horizontal one. The corresponding transformation given by the waveplate can be expressed as

$$\begin{bmatrix} \hat{a}_H^\dagger(m) \\ \hat{a}_V^\dagger(m) \end{bmatrix}_{(out)} = \begin{bmatrix} 1 & 0 \\ 0 & e^{-i\phi} \end{bmatrix} \begin{bmatrix} \hat{a}_H^\dagger(m) \\ \hat{a}_V^\dagger(m) \end{bmatrix}_{(in)}, \quad (23)$$

where the index u in $S(u, \phi)$ specifies the column and row associated with $\hat{a}_V^{\dagger(m)}$.

The transformation $W(u, v, \omega)$ can be realized differently depending on whether the modes involved refer to different polarizations of the same rail, or two spatial modes on different rails. In the first case, a simple rotation equal to ω of the coordinate system on the polarization plane realizes the transformation, i.e.,

$$\begin{bmatrix} \hat{a}_H^{\dagger(m)} \\ \hat{a}_V^{\dagger(m)} \end{bmatrix}_{(out)} = \begin{bmatrix} \cos(\omega) & \sin(\omega) \\ -\sin(\omega) & \cos(\omega) \end{bmatrix} \begin{bmatrix} \hat{a}_H^{\dagger(m)} \\ \hat{a}_V^{\dagger(m)} \end{bmatrix}_{(in)}. \quad (24)$$

In this case, the indices u, v specify the columns and rows of $\hat{a}_H^{\dagger(m)}, \hat{a}_V^{\dagger(m)}$ respectively. If a mixing between two different spatial modes is required, a beam splitter (BS) with the appropriate transmissivity and reflectivity may be used. The transmissivity and reflectivity may even depend on the polarization, and in this case a partially polarizing beam splitter (PPBS) is required to realize the transformation

$$\begin{bmatrix} \cos(\omega_H) & 0 & \sin(\omega_H) & 0 \\ 0 & \cos(\omega_V) & 0 & \sin(\omega_V) \\ -\sin(\omega_H) & 0 & \cos(\omega_H) & 0 \\ 0 & -\sin(\omega_V) & 0 & \cos(\omega_V) \end{bmatrix} \quad (25)$$

from the input to the output creation operators enlisted in the column $[\hat{a}_H^{\dagger(m)}, \hat{a}_V^{\dagger(m)}, \hat{a}_H^{\dagger(n)}, \hat{a}_V^{\dagger(n)}]^T$. In this case, we are actually implementing the transformation $W(u, v, \omega_H) \cdot W(u', v', \omega_V)$, where u, v point at the coefficients of the horizontal polarizations and u', v' at those of the vertical ones. When $\omega_H = \omega_V$, we recover the transformation of a BS. An extreme example of PPBS is the polarizing beam splitter (PBS), which completely transmits the horizontal polarizations and reflects the vertical polarizations, and corresponds to the transformation (25) with $\omega_H = 0, \omega_V = \pi/2$.

In order to obtain the implementation of (17), we follow the sequence of the unitary transformations $S(u, \phi), W(u, v, \omega)$ from right to left and compose in a cascade the corresponding implementations. Two possible implementations arise, a *direct* one and a *folded* one, which are the topic of the next sections.

D. Direct scheme

The *direct* implementation is designed following the sequence of GR in Eq. (17). Figure 1 depicts the scheme for $M = 8$, where the optical network and the photon counters can be clearly recognized.

The scheme presents an *initial block* implementing the unitaries $W(1, 2, \pi/4)$ and $S(2, \pi/2)$. The qubit to be measured is defined on the Cartesian coordinate system of the polarization plane, which is rotated by $\pi/4$ in order to implement $W(1, 2, \pi/4)$. In Fig. 1, such a rotation is indicated with a curved arrow.

The optical modes $H^{(1)}, V^{(1)}$ must then go through a quarter-wave plate which realizes $S(2, \pi/2)$. The wave-plate, indicated in Fig. 1 with a slim rectangular box, is aligned with the new coordinate system, and the same holds for the following components.

The decomposition (17) highlights a structure for the matrices following the initial block. In particular, the GR can be grouped in triplets which work on the same group of modes, e.g.

$$W(3, 4, \omega_{34}) \cdot W(2, 4, \omega_{24}) \cdot W(1, 3, \omega_{13}). \quad (26)$$

The same holds if we add $2k, k = 0, \dots, \frac{M}{2} - 2$ to the indices of the modes, and employing the angles $\omega_{34} = \pi + \frac{\pi}{M}$ and $\omega_{24} = \omega_{13} = \arctan \sqrt{(M-2-2k)/2}$.

This observation suggests a modular implementation of the triplet, which is repeated several times. The modular block is shown within the dashed line in Fig. 1.

In general, the unitaries $W(2, 4, \omega_{24}) \cdot W(1, 3, \omega_{13})$ may be implemented with a PPBS realizing (25) with $\omega_H = \omega_{13}, \omega_V = \omega_{24}$, where the horizontal creation operators have indices 1, 3 and the vertical ones have indices 2, 4. However, since $\omega_H = \omega_V = \omega_{24} = \arctan \sqrt{(M-2-2k)/2}$, a BS suffices to implement the transformation. After this, two of the outgoing modes go to a PBS to be separated into horizontal and vertical polarization modes, and then on to photon counters to record a possible click. The other two outgoing modes are mixed with a rotation of the polarization plane, realizing the unitary $W(3, 4, \omega_{34})$ as in (24), with $\omega = \omega_{34} = \pi + \frac{\pi}{M}$.

Note that the actual transformation implemented by the BS followed by the rotation of the polarization plane would be (supposing $k = 1$)

$$\begin{bmatrix} \sqrt{\frac{2}{M}} & 0 & \sqrt{\frac{M-2}{M}} & 0 \\ 0 & \sqrt{\frac{2}{M}} & 0 & \sqrt{\frac{M-2}{M}} \\ \sqrt{\frac{M-2}{M}} \cos(\frac{\pi}{M}) & \sqrt{\frac{M-2}{M}} \sin(\frac{\pi}{M}) & -\sqrt{\frac{2}{M}} \cos(\frac{\pi}{M}) & -\sqrt{\frac{2}{M}} \sin(\frac{\pi}{M}) \\ -\sqrt{\frac{M-2}{M}} \sin(\frac{\pi}{M}) & \sqrt{\frac{M-2}{M}} \cos(\frac{\pi}{M}) & \sqrt{\frac{2}{M}} \sin(\frac{\pi}{M}) & -\sqrt{\frac{2}{M}} \cos(\frac{\pi}{M}) \end{bmatrix}. \quad (27)$$

However, two of the input modes of the PPBS are vacuum states, and the effective transformation from the coefficients of $[\hat{a}_H^{\dagger(m)}, \hat{a}_V^{\dagger(m)}]^T$ to those of $[\hat{a}_H^{\dagger(m)}, \hat{a}_V^{\dagger(m)}, \hat{a}_H^{\dagger(n)}, \hat{a}_V^{\dagger(n)}]^T$ results

$$\begin{bmatrix} \hat{a}_H^{\dagger(m)} \\ \hat{a}_V^{\dagger(m)} \\ \hat{a}_H^{\dagger(n)} \\ \hat{a}_V^{\dagger(n)} \end{bmatrix} = \begin{bmatrix} \sqrt{\frac{2}{M}} & 0 \\ 0 & \sqrt{\frac{2}{M}} \\ \sqrt{\frac{M-2}{M}} \cos(\frac{\pi}{M}) & \sqrt{\frac{M-2}{M}} \sin(\frac{\pi}{M}) \\ -\sqrt{\frac{M-2}{M}} \sin(\frac{\pi}{M}) & \sqrt{\frac{M-2}{M}} \cos(\frac{\pi}{M}) \end{bmatrix} \begin{bmatrix} \hat{a}_H^{\dagger(m)} \\ \hat{a}_V^{\dagger(m)} \end{bmatrix}. \quad (28)$$

The horizontal and vertical polarizations of mode m then goes to a PBS followed by two photon counters, while those in mode n go to the next modular block, or to additional photon counters in the case of the last module.

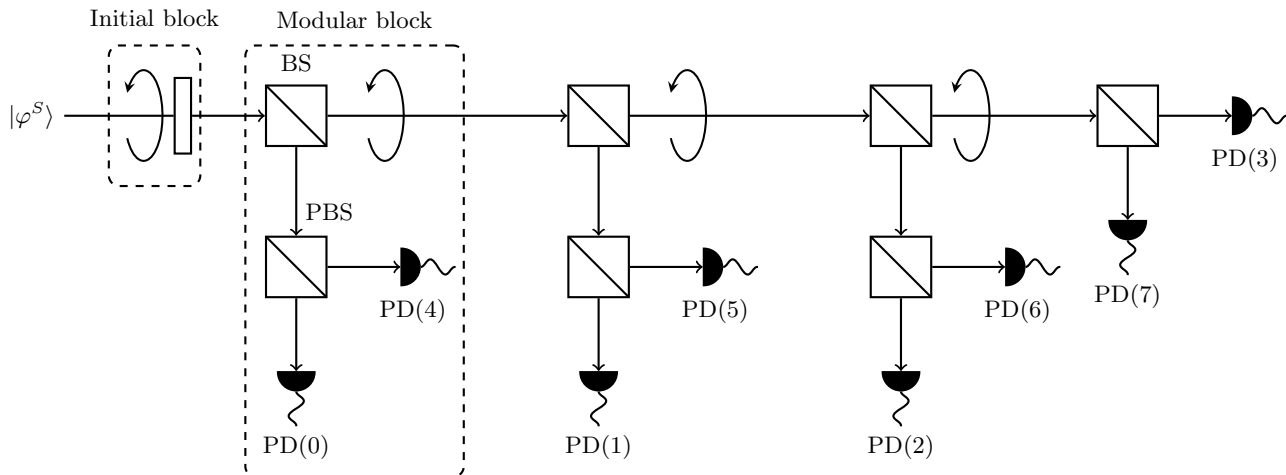


FIG. 1. Direct scheme for $M=8$. The qubit $|\varphi^S\rangle$ to be measured enters the optical network from the left and traverses the optical network to give the correct outcome probability. The initial block and a modular block, which is then repeated three times, are enclosed within dashed lines. Each modular block is composed by a BS, a PBS, two photon counters and a polarization plane rotation (depicted with a curved arrow). Each block has two ingoing modes coming from the previous block and two ingoing auxiliary modes in the vacuum state. Two outgoing modes of the BS are directed to the PBS and then to photon counters, while the other two outgoing modes are directed towards the polarization plane rotation and then to the next block. A click in the photon counter $PD(k)$ corresponds to the projection on $P_k = Z^\dagger |e_k^H\rangle \langle e_k^H| Z$ in the extended Hilbert space.

As a side note, we would like to point out that, in general, photonic implementations with BS require the rails to be swapped and brought close in order to perform the unitary operation on adjacent modes. The direct scheme, as well as the folded scheme, are free of this issue as can be seen from the schematics of Figs. 1 and 2. This is also true for arbitrarily high M since this property originates from the pattern of GR triplets in the decomposition of Z^\dagger and their modular implementation with a BS and a polarization plane rotation.

E. Folded scheme

The folded scheme is a variation of the direct scheme which comes from the following considerations.

Firstly, an experimental implementation of the direct scheme requires a number of photon counters equal to the number of outcomes M , which may become highly expensive to realize if a fine resolution of the phase is required, i.e., a large number M . It is therefore worthwhile exploring the possibility of reducing the number of devices required.

Secondly, the photon counters and the modular blocks in general are not “used” at the same time, but at different times as the photon will click later in $PD(k)$ with respect to $PD(0)$. This opens up the possibility to exploit “recursive” schemes that reuse the same modular block in different time slots.

The folded scheme is obtained by putting a delay line after the first modular block, connecting the output modes of this block to the input modes of the PPBS, effectively “folding” all the blocks onto the first one. Fig. 2

shows a possible implementation of the scheme.

Note that since the parameters ω_H , ω_V change from one modular block to another, a time-varying BS is required, which may be realized with an interferometer with the appropriate phase shift on one arm. This interferometer is singled out inside the dashed enclosure in Fig. 2.

The photon to be measured enters the loop and in the following $M/2$ time slots (each lasting a round trip time in the delay line) it exits towards the PBS and the photon counters. The outcome depends both on the polarization and the time slot, and it corresponds to k and $k+M/2$ for a click recorded in the $(k+1)$ -th time slot in the photon counter associated respectively with the horizontal and vertical polarization.

A comment on the experimental feasibility of these schemes is in order. As a matter of fact, the direct scheme can straightforwardly be realised with bulk optics or in integrated optical circuits. On the other hand, the folded scheme requires a careful design of the delay line. In particular, its length defines the time slot where a photon can be recorded at the photon counters, and must at least amount to the temporal span of the single photon plus the time required to the time-varying BS to adjust its parameters. This latter duration is the slower constraint, with commercial devices that reports switching frequencies of the order of tens of MHz in their datasheet. The resulting length for the delay line is of the order of tens of meters, which are feasible to realize in a lab. The dead time of photon counter, which may blind successive time slots, does not impact the current measurement, thought it may affect the time slots in the following one. This can be solved by imposing an idle time interval between con-

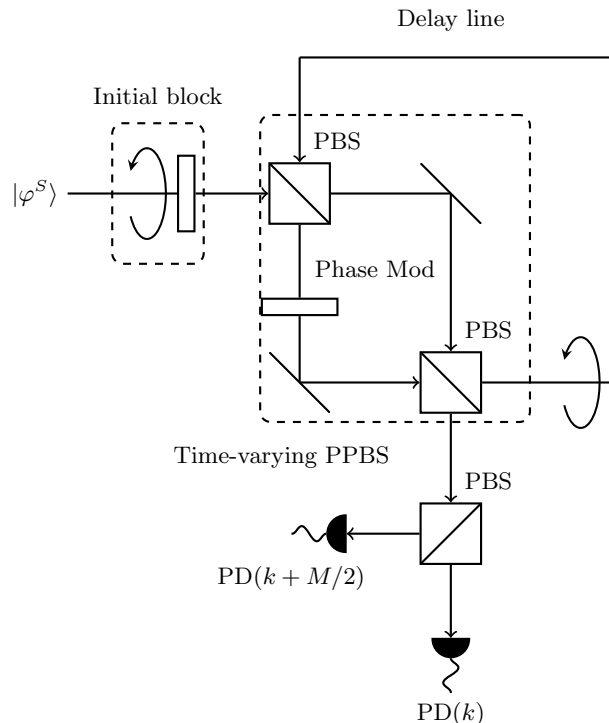


FIG. 2. Folded scheme for the phase measurement. The qubit $|\varphi^S\rangle$ to be measured travels through an initial block and enters an optical loop defined by the interferometer and the delay line. The initial block and the interferometer, which implements a time-varying BS, are enclosed within dashed lines. The optical loop, composed by the interferometer, PBS, photon counters and the polarization-plane rotation (depicted with a curved arrow) corresponds to the modular block of the direct scheme. The photon exits the loop via the second BS in the interferometer, and its polarizations are splitted with a PBS and directed to photon counters. The measurement outcome k [or $k + M/2$] is obtained when a click in $\text{PD}(k)$ [$\text{PD}(k + M/2)$] is recorded in the $(k + 1)$ -th time slots, which is defined as the time interval that takes the photon to travel in the loop.

secutive measurements, which reduces the overall rate of measurements that can be performed. However, for a proof-of-principle experimental test this is usually not an issue.

IV. CONCLUSIONS

In conclusion, we have addressed the optical implementation of POVM corresponding to the optimal M -outcomes discrimination of the polarization state of a single photon. In particular, we have found an explicit Naimark extension and optical implementation for any $M = 2^N$, $N > 1$, so that the resolution of the estimated phase can be arbitrarily small.

The measurement scheme has been devised to estimate the phase of the polarization of a single photon. The single photon passes through an optical network towards a set of photon counters, providing information about which path was taken, depending on its polarization. The optical network is defined by the unitary obtained from the projectors, and it is realized as a sequence of modular blocks that reflects the structure of the unitary decomposition in GR. Each block is a combination of beam splitters and waveplates that act on multiple polarization modes. The photon counters are placed at the outgoing

modes and at each recorded click they assign the corresponding outcome.

We have provided the analytical expression for both the Naimark extension and its decomposition in GR, and we have proposed an implementation for the measurement scheme of the polarization, but other phase measurements can in principle be realized. Our results pave the way for realistic implementations of the canonical phase POVM for single-photon states and for extension to high-dimensional Hilbert spaces.

ACKNOWLEDGMENTS

N. Dalla Pozza thanks G. Vallone, M. Avesani and J. Tinsley for useful discussions and comments. M. G. A. Paris is member of GNFM-INdAM and thanks S. Olivares and S. Cialdi for discussions.

-
- [1] N. Gisin and R. Thew, *Nature Photonics* **1**, 165 (2007).
- [2] L. Gyongyosi, S. Imre, and H. V. Nguyen, *IEEE Communications Surveys & Tutorials* **20**, 1149 (2018).
- [3] N. Gisin, G. Ribordy, W. Tittel, and H. Zbinden, *Reviews of Modern Physics* **74**, 145 (2002).
- [4] H.-K. Lo, M. Curty, and K. Tamaki, *Nature Photonics* **8**, 595 (2014).
- [5] C. Elliott, *New Journal of Physics* **4**, 46 (2002).
- [6] S. Lloyd, J. H. Shapiro, F. N. C. Wong, P. Kumar, S. M. Shahriar, and H. P. Yuen, *ACM SIGCOMM Computer Communication Review* **34**, 9 (2004).
- [7] H. J. Kimble, *Nature* **453**, 1023 (2008).
- [8] E. Knill, R. Laflamme, and G. J. Milburn, *Nature* **409**, 46 (2001).
- [9] R. Raussendorf and H. J. Briegel, *Physical Review Letters* **86**, 5188 (2001).
- [10] T. C. Ralph, *Reports on Progress in Physics* **69**, 853 (2006).
- [11] J. Chen, J. L. Habif, Z. Dutton, R. Lazarus, and S. Guha, *Nature Photonics* **6**, 374 (2012).
- [12] C. Pfister, M. A. Rol, A. Mantri, M. Tomamichel, and S. Wehner, *Nature Communications* **9**, 27 (2018).
- [13] A. Boaron, G. Boso, D. Rusca, C. Vulliez, C. Autebert, M. Caloz, M. Perrenoud, G. Gras, F. Bussièrès, M.-J. Li, D. Nolan, A. Martin, and H. Zbinden, *Physical Review Letters* **121**, 190502 (2018).
- [14] Q. Zhang, F. Xu, Y.-A. Chen, C.-Z. Peng, and J.-W. Pan, *Optics Express* **26**, 24260 (2018).
- [15] A. Dahlberg and S. Wehner, *Quantum Science and Technology* **4**, 015001 (2018).
- [16] S. Wehner, D. Elkouss, and R. Hanson, *Science* **362**, eaam9288 (2018).
- [17] S. Takeda and A. Furusawa, *APL Photonics* **4**, 060902 (2019).
- [18] H.-J. Briegel, W. Dür, J. I. Cirac, and P. Zoller, *Physical Review Letters* **81**, 5932 (1998).
- [19] K. Azuma, K. Tamaki, and H.-K. Lo, *Nature Communications* **6**, 6787 (2015).
- [20] T. C. Ralph, A. P. Lund, and H. M. Wiseman, *Journal of Optics B: Quantum and Semiclassical Optics* **7**, S245 (2005).
- [21] M. G. Thompson, A. Politi, J. C. F. Matthews, and J. L. O'Brien, *IET Circuits, Devices Systems* **5**, 94 (2011).
- [22] J. L. O'Brien, A. Furusawa, and J. Vuckovic, *Nature Photonics* **3**, 687 EP (2009), review Article.
- [23] T. E. Northup and R. Blatt, *Nature Photonics* **8**, 356 (2014).
- [24] E. Diamanti, H.-K. Lo, B. Qi, and Z. Yuan, *npj Quantum Information* **2**, 16025 (2016).
- [25] A. Shenoy-Hejamadi, A. Pathak, and S. Radhakrishna, *Quanta* **6**, 1 (2017).
- [26] S. Pirandola, U. L. Andersen, L. Banchi, M. Berta, D. Bunandar, R. Colbeck, D. Englund, T. Gehring, C. Lupo, C. Ottaviani, J. Pereira, M. Razavi, J. S. Shaari, M. Tomamichel, V. C. Usenko, G. Vallone, P. Villoresi, and P. Wallden, "Advances in quantum cryptography," (2019), arXiv:1906.01645.
- [27] P. Kok, W. J. Munro, K. Nemoto, T. C. Ralph, J. P. Dowling, and G. J. Milburn, *Reviews of Modern Physics* **79**, 135 (2007).
- [28] H. Krovi, *Nanophotonics* **6**, 531 (2017).
- [29] M. A. Naïmark, *Izv. Akad. Nauk SSSR, Ser. Mat.* **7**, 285 (1943).
- [30] N. I. Akhiezer and I. M. Glazman, *Theory of Linear Operators in Hilbert Space (Dover Books on Mathematics)* (Dover Publications, 1993).
- [31] C. W. Helstrom, *International Journal of Theoretical Physics* **8**, 361 (1973).
- [32] C. W. Helstrom, *Quantum detection and estimation theory*, Math. Sci. Eng. (Academic Press, New York, NY, 1976).
- [33] A. S. Holevo, *Statistical Structure of Quantum Theory* (Springer Berlin Heidelberg, 2001).
- [34] A. Peres, *Foundations of Physics* **20**, 1441 (1990).
- [35] B. He, J. A. Bergou, and Z. Wang, *Phys. Rev. A* **76**, 042326 (2007).
- [36] J. A. Bergou, *Journal of Modern Optics* **57**, 160 (2010), <https://doi.org/10.1080/09500340903477756>.
- [37] M. G. A. Paris, *The European Physical Journal Special Topics* **203**, 6 (2017).
- [38] N. Dalla Pozza and M. G. A. Paris, *International Journal of Quantum Information* **15**, 1750029 (2017).
- [39] Since the algorithm enlarges the size of the Hilbert space \mathcal{H} only when necessary, the size of \mathcal{H}_A is only determined at the end.
- [40] By Eq. (9), the choice $\rho_A = |e_1^A\rangle\langle e_1^A|$ imposes that the first entries of Z_k are equal to X_k .
- [41] R. A. Horn and C. R. Johnson, *Matrix Analysis*, 2nd ed. (Cambridge University Press, New York, NY, USA, 2012).
- [42] On the contrary, linear mixing between annihilation operators and creation operators require nonlinear optical interactions, as it results from squeezing transformations.
- [43] M. Reck, A. Zeilinger, H. J. Bernstein, and P. Bertani, *Phys. Rev. Lett.* **73**, 58 (1994).